Progress In Electromagnetics Research Letters, Vol. 60, 95–100, 2016

Broadband Transition from Microstrip Line to Waveguide Using a Radial Probe and Extended GND Planes for Millimeter-Wave Applications

Azzemi Ariffin*, Dino Isa, and Amin Malekmohammadi

Abstract—A broadband microstrip line-to-waveguide (MSL-to-WG) transition is developed for E-band applications. In order to achieve a sufficient and broadband coupling between the microstrip line (MSL) and waveguide (WG), a radial electric probe at the end of the MSL and extended ground (GND) planes on the dielectric substrate are proposed. Results are compared against a simple transition (S-Tr) with a straight electric probe. For the case of operational bandwidth (BW) for an input return loss (S_{11}) below -20 dB, the proposed transitions using the radial probe and extended GND planes show the BW enhancement of 33.8% and 61.9%, respectively, compared to the S-Tr. The proposed and simple transitions were fabricated on a low-loss liquid crystal polymer (LCP) dielectric substrate. The measured bandwidth (BW) for S_{11} below -10 dB of the proposed transition is over 28 GHz, which is satisfied at all test frequencies from 67 to 95 GHz. Its measured insertion loss can be analyzed as -1.33 and -1.41 dB per transition at 70 and 80 GHz, respectively, considering the loss contribution of the cable adapter and waveguide transition.

1. INTRODUCTION

Millimeter-wave (MMW) technology has been recognized as having potential for emerging markets and developed for broadband ultra-high-speed wireless communication systems such as broadband radio links for the backhaul networking [1] of cellular base stations, Giga wireless LAN, Gigabit Ethernet networks, 77 GHz automotive radar systems [2] and inter-vehicle communications.

Many kinds of wireless systems have been developed by using MMW bands. Especially, E-band including 71∼76 and 81∼86 GHz band can offer competitive and compelling alternative, compared to other MMW, in terms of wide available spectrum, low-loss propagation characteristics, and effective cost. However, a challenge of a design of very wide-band radio systems has to be overcome. In general, radio systems consist of several types of transmission lines such as a microstrip line (MSL), coplanar waveguide (CPW), and waveguide (WG). Moreover, some outdoor applications [3] require integration of bulky components such as high-gain array or waveguide (WG) antenna, nonplanar filters, waveguides, and connectors. Therefore, wideband transitions [4, 5] between them are required.

In general, a simple electrical probe (E-probe) transition [6] has been used for MMW applications due to its simple design and mode transformation, and it also has a $\lambda/4$ back-short WG on an aperture of a dielectric substrate. However, because of its endemic problem of the narrow bandwidth, its applications have been limited. In order to enhance its bandwidth, various technologies have been developed [7–9]. The mode matching methods using a ridge waveguide impedance transformer [7], quasi-Yagi antenna [8], and probe shifting [9] have been proposed. Although they have demonstrated bandwidth extension, an additional structure such as an air bridge or trenched metal block is needed or design process is rigorous.

Received 8 April 2016, Accepted 11 May 2016, Scheduled 26 May 2016

* Corresponding author: Azzemi Ariffin (azzemi@tmrnd.com.my).

The authors are with the Department of Electrical and Electronic Engineering, Faculty of Engineering, The University of Nottingham, Malaysia Campus, Malaysia.

In this work, a wideband transition from a MSL to WG has been presented for MMW applications. Its bandwidth of 60.81% is broadened by using a radial probe and extended ground planes.

2. DESIGN OF A BROADBAND MICROSTRIP LINE(MSL)-TO-WAVEGUIDE (WG) TRANSITION

The MSL-to-WG transitions were designed and analyzed by using a 3-D Finite Integration Technique (FIT) simulator for E-band applications. The transition is composed of an E-probe, dielectric substrate, and $\lambda_g/4$ short-back WG. λ_g is a guided wavelength. A liquid crystal polymer (LCP) has been used because of low-loss characteristics in the MMW band and its relative dielectric constant, loss tangent and thickness are 3.16, 0.0045, and 100 µm, respectively. A metal (Cu) thickness on the substrate is 8 µm. The WG in this work is WR 12 with a rectangular size of 3.1×1.55 mm^2 for E-band module applications.

Figure 1 shows a configuration of the MSL-to-WG transition using a simple probe. In general, a simple transition (S-Tr) pattern of an electrical probe (E-probe) at the end of MSL on the substrate is shown in Fig. 1(a). The substrate with the S-Tr is attached on the lower WG, and a $\lambda_g/4$ short-back upper WG with a metal cover for short circuit is assembled on the substrate as shown in Fig. 1(b). The length of the upper WG is 700 µm. Leakage due to lateral radiation is suppressed by using vias to connect each other's ground planes on the substrate with the upper and lower WGs. The width of a 50 Ω MSL is 236 µm. In the design model, the MSL and WG are connected to port 1 and port 2, respectively.

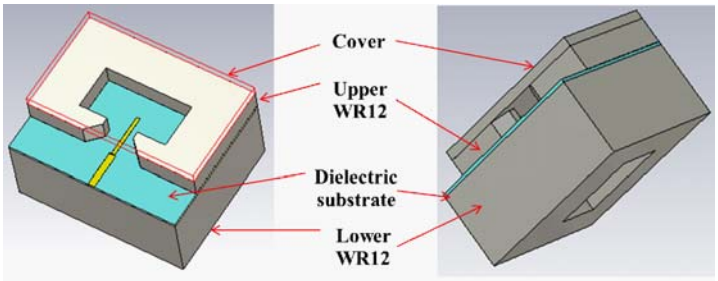

Figure 1. Configuration of a MSL-to-WG transition.

2.1. Design of the E-Probe

In general, a radial stub has been used at the impedance matching networks for the broadband small-signal gain [10]. It can also be utilized for the wideband E-probe. Fig. 2 shows the E-probe patterns for the MSL-to-WG transition using a simple electrical probe (S-probe) (a) and a radial electrical probe (R-probe) (b). For the S-probe, its total length and inserted one are 1,475 and 794 µm, respectively. In the case of R-probe, a R-probe with a length of 321 µm and angle of 90 degrees is designed at the end of an S-probe as shown in Fig. 2(b). Its inserted length is 754 µm, and the length and inserted position are optimized. Its angle is fixed at 90 degrees, considering the operational bandwidth (BW) and the extent of impedance matching. As the angle is decreased, the BW is extended, but impedance matching is a little worse. WG ground patterns of the two transitions are the same.

Figure 3 presents the designed reflection characteristics (S_{11}, S_{22}) and an insertion loss (S_{21}) of the MSL-to-WG transition using the S-probe, compared to the transition using the R-probe. S_{11} and S_{22} are a bit different due to different ports assigned at the MSL and WG. In the case of operational bandwidth (BW) for an input return loss (S_{11}) below −20 dB, 16.46 and 22.03 GHz are observed for the S-probe and R-probe, respectively. The R-probe shows the BW improvement of 33.8%, compared to that of the S-probe, which results from broadband matching characteristics of the radial-probe.

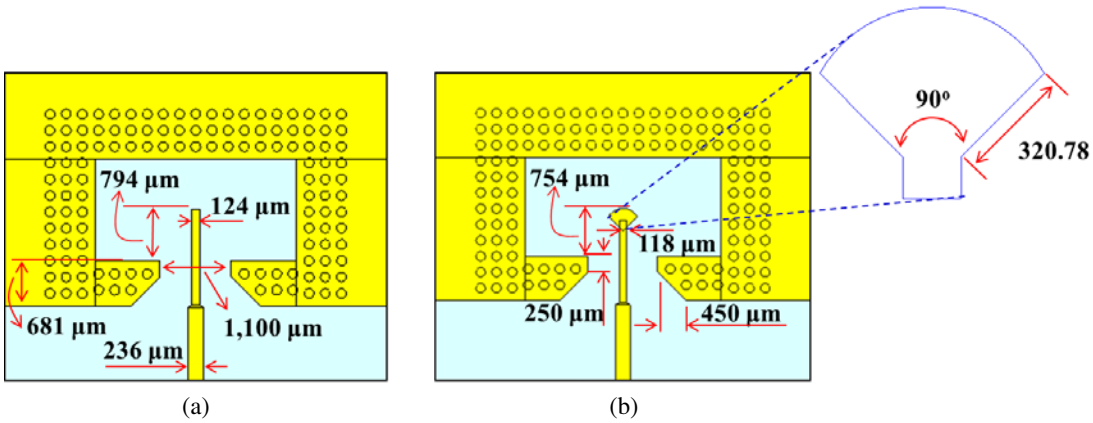

Figure 2. E-probe patterns of an (a) S-probe and (b) R-probe.

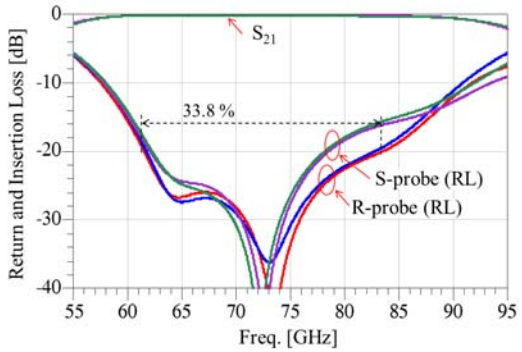

Figure 3. Designed results of the MSL-to-WG transition using the S-probe and R-probe.

2.2. Design of the Extended Ground Plane (eGND) in the Transition

In order to enhance the BW of the transition, extended ground (eGND) planes [11] are inserted into the ground surrounding R-probe, and their widths are optimized. For the eGND at the ground bottom side and changing its width from 100 to 200 μm, the reflection loss (S_{11}) is investigated as shown in Fig. 4(a). By increasing the width, aresonant frequency is increased, and the BW of 23.27 GHz (61.47∼84.74 GHz) is achieved at the eGND width of 160 μm, in spite of a little difference of the BW. After fixing the eGND width at the bottom side, an eGND at the ground upper side is investigated. It can be seen from the simulation results that the width affects the wideband impedance matching to the WG as shown in Fig. 4(b). As its width extends over 17 μm, the impedance matching condition is gradually degenerated, and its width is optimized to 260 μm. In this case, the BW is 26.49 GHz from 60.51 to 87.0 GHz. By inserting eGND planes at the bottom and upper side of the ground surrounding R-probe, the BW is enhanced by 5.63 and 13.84%, respectively, compared to that of the transition using the R-probe. It can be clearly seen that eGND is effective for enhancement of the BW and broad impedance matching of the transition. Compared to the transition with the S-probe, the BW improvement of the transition using the R-probe and eGND is 60.94% from 16.46 to 26.49 GHz

In order to test the fabricated transitions, the MSL-to-WG transitions should be designed in back-to-back configuration. Two MSL ports of two transitions are connected by using a 2,060 μm-long MSL. Fig. 5 presents the simulated results of the proposed transition with the R-probe and eGND in back-to-back type. The BW for S_{11} below −20 dB is 2533 GHz from 61.75 to 87.05 GHz. The BW is shorter than that of the single transition, and S_{11} is a little degraded at 77.14 GHz, due to parasitic reactance of the long MSL. For comparison purpose, two transitions using the S-probe and R-probe are designed and fabricated.

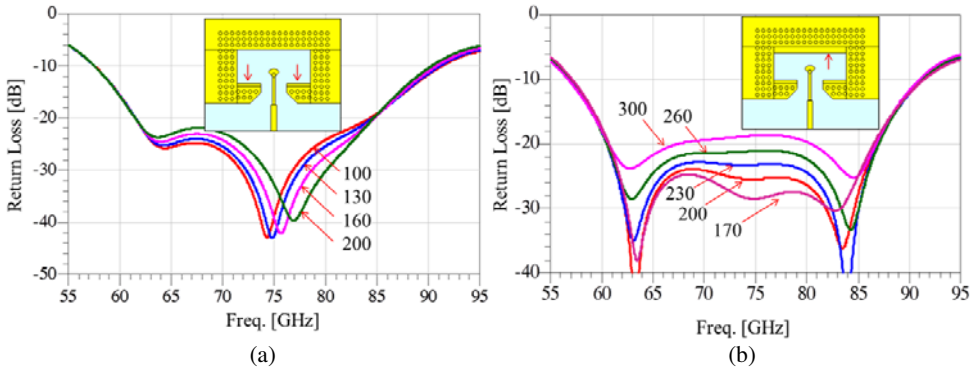

Figure 4. Designed results of the eGND planes (a) at the bottom side and (b) at the upper side of the WG aperture [Insets of (a) and (b) are the layout of the transition with eGND, respectively].

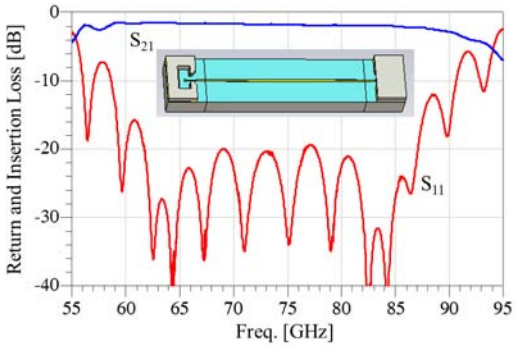

Figure 5. Simulated results of the MSL-to-WR12 transition in back-to-back structure [The inset is a 3 dimensional structure for simulation of the transition in back-to-back type and the closure is open in the left transition].

3. FABRICATION AND TEST RESULTS

The designed transitions were fabricated by using a commercial printed circuit board (PCB) foundry service. Fig. 6 shows the transitions fabricated on the dielectric substrate in a back-to-back type (a), metal patterns (b), and the upper WG (c) without a cover. WGs are made from Aluminum (Al) block. The patterned metal on the PCB is Cu/Ni/Au (15/3/0.3 µm). All fabricated transition components including the PCB and WGs were assembled by using a conductive epoxy and screws.

In order to test and analyze the fabricated transitions, at first, loss characteristics of a 20.6 mm long and 236 µm-wide MSL, an adapter and WG transition should be measured as shown in Fig. 7. Fig. 7(a) presents the measured results of a 50 Ω MSL fabricated on the LCP substrate by using on-wafer probing on a probe station. At all the test frequencies, the input return loss (RL, S_{11}) is below −10 dB. The insertion losses (IL, S_{21}) of −2.76 and −3.18 dB are observed at 70 and 80 GHz, respectively. Connections of a WG adapter (1.0 mm cable-to-WR10) to a WG transition (WR10-to-WR12) are checked from 67 to 95 GHz, because 1.0 mm cables of a vector network analyzer (VNA) and WR12 WG-type ports of the fabricated transition should be interconnected for the transition test. The test results are shown in Fig. 7(b). S_{11} is less than −10 dB at all test frequencies, and S_{21} at 70 and 80 GHz are −2.38 and −2.00 dB, respectively.

Figure 8 presents a test set-up of the fabricated MSL-to-WR12 WG transitions using the R-probe and eGND planes in back-to-back type (a) and its tested loss characteristics (b), compared to the S-probe. The return loss (S_{11}) and insertion one (S_{21}) are degraded compared to the simulated ones, because of high-loss connection including two adapters and WG transitions. In the case of R-probe, its

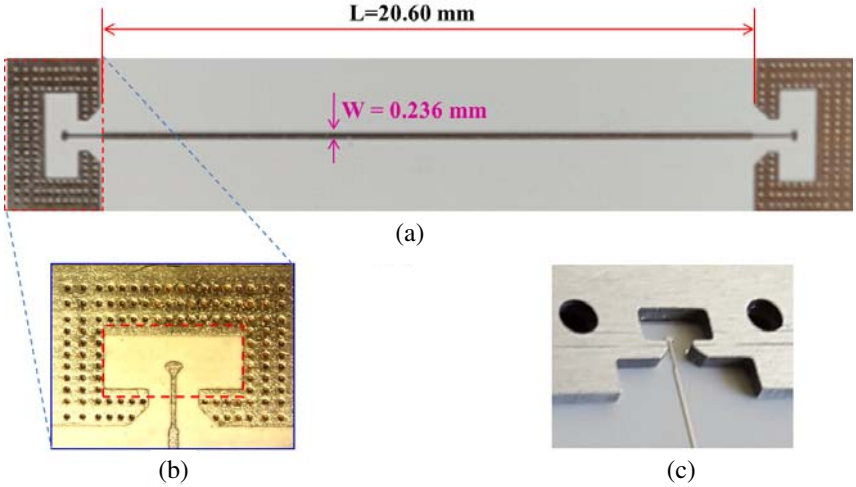

Figure 6. Fabricated transitions in (a) a back-to-back structure, (b) metal patterns on the LCP substrate, and (c) upper WG.

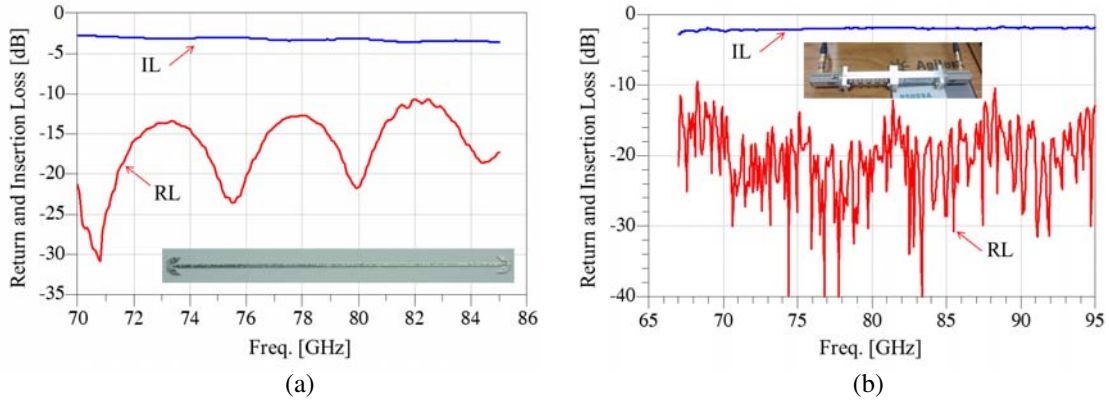

Figure 7. Measured return and insertion loss of a (a) MSL and (b) connections of a cable-to-WG adapter and WG transition [Inset of (a) and (b) are the fabricated 20.6 mm-long MSL and connections of cable-to-WG adapters and WR10-to-WR12 transitions, respectively].

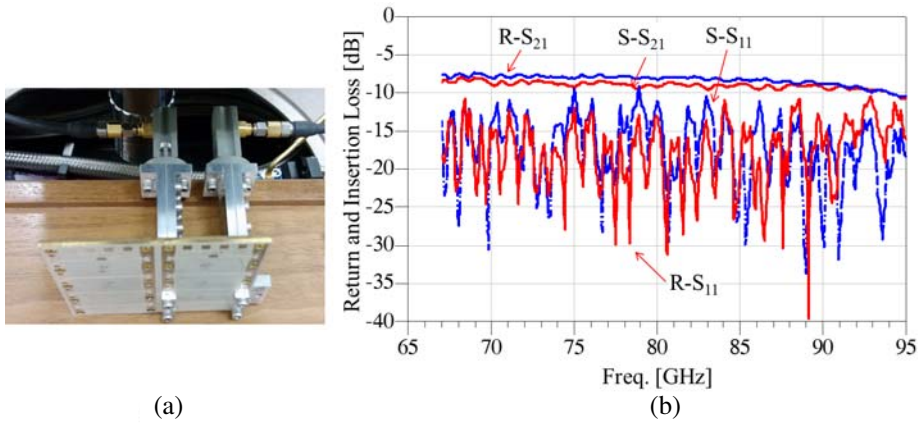

Figure 8. A test set-up of the fabricated MSL-to-WR12 WG transitions using the R-probe and eGND planes in (a) back-to-back type and (b) its measured results [R- and S-: Transition with R-probe and S-probe, respectively].

S_{11} shows less than -10 dB at all test frequencies from 67 to 95 GHz. S_{11} of -8.03 and -8.26 dB are obtained at 70 and 80 GHz, respectively. For the S-probe, S_{21} of -8.88 and -9.24 dB is tested at 70 and 80 GHz, respectively, which is degraded by 0.8 and 1 dB, respectively, compared to the R-probe. This insertion loss includes the loss component from the long MSL, cable-to-WG adapter, and WG transition. Considering these loss components, the transition with the R-probe loss can be analyzed as -1.33 and -1.41 dB per transition at 70 and 80 GHz, respectively.

4. CONCLUSION

A broadband of vertical MS-to-WG transition has been presented for E-band module applications. In this transition, the radial-type probe and extended ground (eGND) planes on the dielectric substrate were proposed. Compared to the ordinary transition using the simple probe, the operational BW of the proposed transition was improved by 33.8% and 61.9% by using the R-probe and optimum extension width of the eGND, respectively. In the final design of the transition, the BW of 26.65 GHz has been obtained from 60.50 to 87.15 GHz. This designed transition was fabricated on an LCP substrate. The fabricated transition was measured by using several adapters and WG transitions. Its measured operational BW for S_{11} below -10 dB was over 28 GHz at all test frequencies from 67 to 95 GHz. The measured insertion loss can be analyzed as -1.33 and -1.41 dB per a transition at 70 and 80 GHz, respectively, by considering the loss contribution of the cable-to-WG adapters and WG transitions.

REFERENCES

1. Asif, S. Z., "E-band microwave radios for mobile backhaul," *I. J. Wireless and Microwave Technologies*, Vol. 4, 37–46, 2015.
2. Gresham, I., N. Jain, T. Budka, A. Alexanian, N. Kinayman, B. Ziegner, S. Brown, and P. Staecker, "A compact manufacturable 76–77- GHz radar module for commercial ACC applications," *IEEE Transactions on Microwave Theory and Techniques*, Vol. 49, 44–58, 2001.
3. Mehrpouyan, H., M. Khanzadi, M. Matthaiou, A. Sayeed, R. Schober, and Y. Hua, "Improving bandwidth efficiency in e-band communication systems," *IEEE Communications Magazine*, Vol. 52, 121–128, 2014.
4. Aliakbarian, H., A. Enayati, G. A. E. Vandenbosch, and W. De Raedt, "Novel low-cost end-wall microstrip-to-waveguide splitter transition," *Progress In Electromagnetics Research*, Vol. 101, 75–96, 2010.
5. Dong, J., T. Yang, Y. Liu, Z. Yang, and Y. Zhou, "Broadband rectangular waveguide to GCPW transition," *Progress In Electromagnetics Research Letters*, Vol. 46, 107–112, 2014.
6. Shih, Y.-C., T.-N. Ton, and L. Q. Bui, "Waveguide-to-microstrip transitions for millimeter-wave applications," *IEEE MTT-S International Microwave Symposium Digest*, 473–475, 1988.
7. Yano, H. Y, A. Abdelmonem, J. F. Liang, and K. A. Zaki, "Analysis and design of microstrip to waveguide transition," *IEEE Transactions on Microwave Theory and Techniques*, Vol. 42, 2371–2379, 1994.
8. Kaneda, N., Y. Qian, and T. Itoh, "A broad-band microstrip-to-waveguide transition using quasi-Yagi antenna," *IEEE Transactions on Microwave Theory and Techniques*, Vol. 47, 2562–2567, 1999.
9. Sakakibara, K., M. Hirono, N., Kikuma, and H. Hirayama, "Broadband and planar microstrip-to-waveguide transitions in millimeter-wave band," *International Conference on Microwave and Millimeter Wave Technology (ICMMT)*, Vol. 3, 1278–1281, 2008.
10. Lee, Y. C. and C. S. Park, "A compact broadband PHEMT MMIC power amplifier for K through Ka-band applications," *Int. J. Electron. Commun. (AEU)*, Vol. 57, 1–4, 2003.
11. Marcuvitz, N., *Waveguide Handbook*, Chapter 5, IEE Press, London, U.K., 1993.